Journal of Ultrafine Grained and Nanostructured Materials
https://jufgnsm.ut.ac.ir
Vol. 57, No.2, December 2024, pp. 168-176
Print ISSN: 2423-6845 Online ISSN: 2423-6837
DOI: 10.22059/jufgnsm.2024.02.07

Influence of P/M process parameters on microstructure and hardness of Al-Al_3Ni composites synthesized in-situ via reactive sintering

Farshad Akhlaghi*, Fatemeh Abedini

School of Metallurgy and Materials Engineering, College of Engineering, University of Tehran
P.O.Box: 11155-4563, Tehran, Iran.

Recieved: 14 November 2024; Accepted: 20 November 2024

**Corresponding author, E-mail:* fakhlagh@ut.ac.ir

ABSTRACT

Al-Al_3Ni composites due to their high strength, creep resistance, fatigue resistance, good ductility, adequate toughness, high corrosion resistance and hardness have gained considerable attention in recent years. In the present investigation, powder metallurgy (PM) method was used to in-situ produce Al-Al_3Ni composites. Commercially pure aluminum powders (63-125 µm) and the same sized pure nickel powders used as starting materials. The Al/Ni powder mixtures with different Ni contents subjected to cold pressing and then sintering at different temperatures for various times. Samples of Al powders without Ni addition were also prepared using identical procedures as for Al/Ni composites to serve as the reference samples. In order to increase effectiveness of interaction between Al and Ni during sintering, Ni powders subjected to high-energy ball milling. The increased milling time of Ni particles from 1.5h to 6h resulted in progressive reaction between Ni flakes and spherical Al particles presented in Al-20wt.% Ni samples which was sintered at 655˚C for 15min. This was accompanied by the increased content of hard Al_3Ni phase and thereby continuous increased hardness of composites. The XRD results confirmed that sintering at 655˚C of the Al/Ni powder compact containing 15wt.% of ball-milled Ni resulted in complete reaction and Al-Al_3Ni eutectic formed without any unreacted Ni. The porosity level of the samples increased with increasing percentage of Al_3Ni phase in the matrix. Brinell hardness values of all the composite samples were higher than that of their reference counterpart. The Al-20wt.% Ni sample prepared by milled Ni exhibited the maximum hardness value being almost three times of that of the reference sample. However, the increased content of milled Ni to 25wt.% resulted in some unreacted Ni particles in the matrix as was confirmed by XRD studies.

Keywords: *Al-Al_3Ni Composites, In-situ method, Powder metallurgy, Ball milling, Sintering, Hardness, XRD, OM, SEM.*

1. Introduction

Among metal matrix composites (MMCs), aluminum matrix composites have received much attention due to their low density, low cost compared to other light alloys such as lithium and titanium as well as good properties such as strength, flexibility and corrosion resistance [1-3]. The processing methods of these composites can be broadly divided into two methods of ex-situ and in-situ techniques. In ex-situ processes, the second phase material is initially prepared and then incorporated in the matrix using a specified process such as casting or powder metallurgy. In these processes, the distribution of the second phase in the matrix is usually non-uniform and this problem results in inferior strength and toughness of the produced composite. Another drawback for ex-situ methods is incident of distractive chemical reactions at the reinforcement/matrix interface, weak bonding due to impurities on the surface of reinforcing phase and its imperfect wettability with the matrix causing inferior mechanical

properties of MMCs [4-6]. In the in-situ processes, the rod shape or lamellar reinforcements are created during plane front solidification of alloys [7]. In addition, the reinforcing particles can be formed by a chemical reaction during processing of the composite. The in-situ formed particles are very fine, thermodynamically stable and well distributed in the matrix alloy and can withstand higher service temperatures. Furthermore, the interface at the reinforcing particle/matrix is clean and causes strong bonding between two adjacent phases resulting in superior mechanical properties specially at elevated temperatures [4, 5, 8-18].

On the other hand, for applications that require low weight, high thermal stability, corrosion resistance and suitable mechanical properties at high temperatures, aluminum intermetallics can be used as structural materials. Al-Ni intermetallics are used in transportation, aerospace and similar industries, but their low ductility and low toughness at room temperature limit their use in engineering design. However, for the MMCs reinforced with intermetallic phases in lamellar or particle forms, this problem is solved. It is reported that Al /Al-Ni composites have properties such as high strength, good fatigue and creep resistance, good ductility and toughness, improved tribological properties and corrosion resistance [19-24]. The Al/Ni equilibrium phase diagram confirms the possibility of formation various intermetallic phases during solidification of Al/Ni alloys [25]. The aluminum matrix composites containing Al_3Ni particles are well known and usually are produced in-situ during eutectic transformation through solidification of Al-Ni alloys. The reinforcing phase in these composites is in the form of lamellar Al-Al_3Ni eutectic. In the present investigation, powder metallurgy (PM) method was used to in-situ produce particulate Al-Al_3Ni composites. The processing parameters of this method were optimized for gaining adequate reaction between Al and Ni powder particles for obtaining superior properties in the resultant composites.

2. Materials and Experimental Procedures

In the present investigation commercially pure, Al powders in the size range of (63-125 μm) and the same sized Ni powders used as starting materials. The SEM images of these powders as shown in Fig. 1 represent respectively semi-spherical and irregular morphologies for the Al and Ni powders.

In order to remove surface impurities, Al and Ni were treated respectively in 0.1% NaOH solution and acetone for 15 min followed by alcohol cleaning and drying before blending. Then the specified amounts of Al and Ni powders were mixed and cold pressed in a steel die at 750 MPa using a 45-ton hydraulic press. In order to optimize the sintering parameters, the green compacts (d=25 mm, h= 20mm), sintered in a tube furnace in air at 640 and/or 655˚C for different times (15-75 min) and subsequently cooled in a power-off furnace to room temperature. For the purpose of comparison, sintered compacts from as-received Al powders were also fabricated using identical compaction and sintering variables. In order to improve the interaction between Al and Ni during sintering, in a number of experiments, flake shaped Ni powders were used. For this purpose, Ni powders were milled for 1.5, 4 and 6h using a planetary ball mill (PM-2400). Milling performed under argon media using hardened steel balls with diameter of 10mm and a hardened stainless steel vial. The rotational speed and the ball-to-powder weight ratio (BPR) were 300 rpm and 15:1, respectively, and 1.5 wt.% of stearic acid (S.A.) was used as the Process Control Agent (PCA) [26]. The SEM studies confirmed that the Ni flakes obtained after 6h milling exhibited the required size and morphology so that these flakes were sieved and the required size range (63-125μm) of these powders were mixed with the as-received Al powders, cold pressed and sintered. The sintered materials were sectioned vertically from their geometrical center along their height. Then they were subjected to standard metallographic procedures and hardness measurements. Microstructure of the samples studied via optical

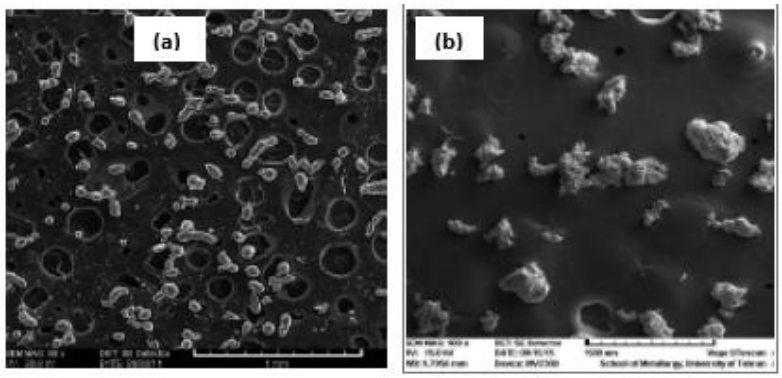

Fig. 1- SEM images of as-received powders a: Al and b: Ni.

microscopy (Olumpus-BX60M), and scanning electron microscopes (CamScanMV2300). The density of the samples was determined using Archimedes principle according to ISO 2738 standard. The samples were precision weighed in distilled water and air using an electronic balance to an accuracy of 0.1 mg. The porosity of samples, were calculated by taking into account their theoretical and measured density values. A high-resolution X-ray diffractometer (Philips-X'pert,) with a rotating copper anode (Cu Kα1, λ= 1.5406 A°) was used for XRD studies. Scans were collected over 2θ range of 10–110° with step size of 0.05° (counting time of 1s per step) and accelerating voltage of 40 kV. XRD patterns were analyzed by using X'Pert High Score software. Hardness measurements were carried out on a Brinell hardness testing machine. The diameter of the penetrator was 2.5mm and the applied load was 30Kg. The average values of at least five measurements conducted on different areas of each sample was considered.

3. Results and Discussions

3.1. Optimization of the sintering time

3.1.1. Microstructure

In order to optimize the sintering time, the Al/Ni powder mixtures containing 15wt.% Ni were sintered at 640˚C for different periods of time. We aimed to investigate the degree of progress of reaction between Al and Ni by employing optical microscopy (OM) and scanning electron microscopy (SEM) studies as well as porosity and hardness measurements. In fact according to Al/Ni equilibrium phase diagram [25], this temperature is almost equal to eutectic transformation temperature of the Al/Ni system which is 639.9 ˚C. The SEM image of the Al-15wt.%Ni green compact before sintering as shown in Fig. 2 confirms the uniform distribution of Ni particles within the matrix alloy.

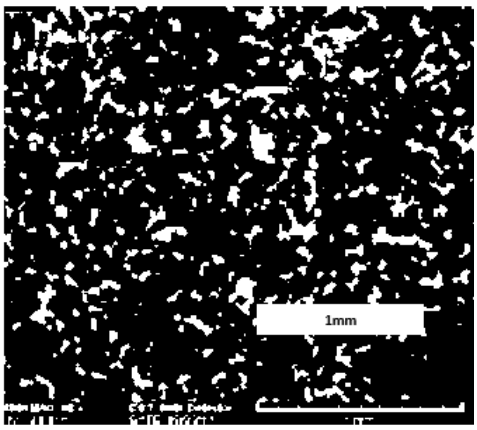

Fig. 2- SEM image of the Al-15wt.%Ni green compact before sintering. The white spots are Ni particles.

The OM images of the polished cross section of the Al-15wt.% Ni samples sintered at 640˚C for 15 and 30 minutes are shown in Figs. 3(a) and 3(b) respectively. These images clearly show the unreacted Ni particles confirming incident of no reaction between Al and Ni during sintering. However sintering for longer durations of 45 and 60 min resulted in formation of Al-Al_3Ni around the Ni particles as shown respectively in the Figs. 4(a) and 4(b). It is clear that the increased sintering time from 45 to 60 min intensified the eutectic reaction at the surface of Ni particles.

The OM and SEM micrographs of the Al-15wt.% Ni sample sintered at 640˚C for 75 minutes are respectively shown in Figs. 5-a and 5-b. These Figs. confirm that Ni particles partially diminished and replaced by eutectic compound. The porous morphology of the Al-Al_3Ni compound as shown in the SEM micrograph of this sample also reported by Lieblich and his co-workers [18] and attributed to unsymmetrical growth of this compound.

3.1.2. Porosity and Hardness

The percentage of porosity of Al-15wt.% Ni samples sintered at 640˚C for different times are shown in Table 1. It can be seen that the increased sintering time resulted in increased porosity level. These results are attributed to the increased volume of Al-Al_3Ni compound for increased sintering temperature as was mentioned earlier. In fact, as shown in Fig5-b, this compound is porous and its increased content results in increased porosity of the sample.

The variation in Brinell hardness of Al-15wt.% Ni composites sintered at 640˚C for different times are shown in Fig. 6. In this Fig. the hardness values obtained for the reference samples sintered at identical conditions as for the composites are also

Table 1- Porosity of Al-15wt.% Ni samples sintered at 640˚C for different times.

Sintering time (min)	Porosity(%)
15	3.1
30	4.5
45	5.1
60	6.5
75	7.3

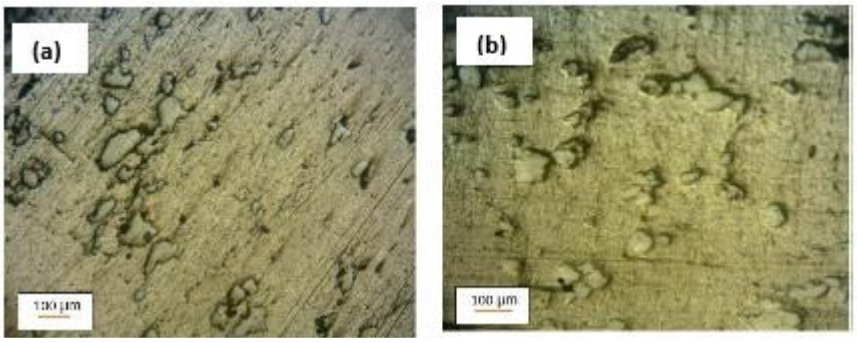

Fig. 3- Optical images of Al-15wt.% Ni samples sintered at 640˚C for a):15 and b):30 minutes.

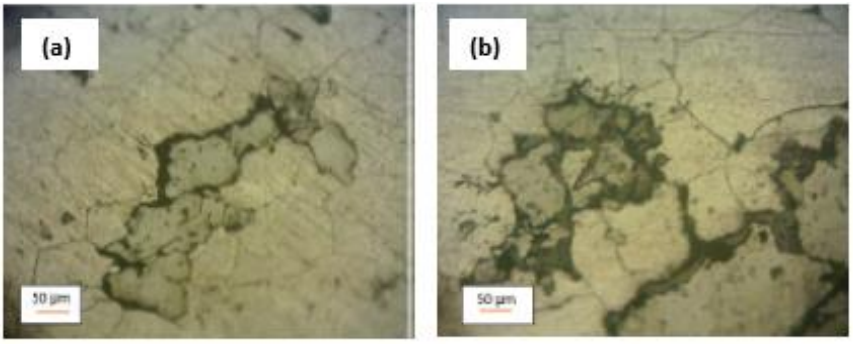

Fig. 4- Optical images of Al-15wt.% Ni samples sintered at 640˚C for a):45 and b):60 minutes.

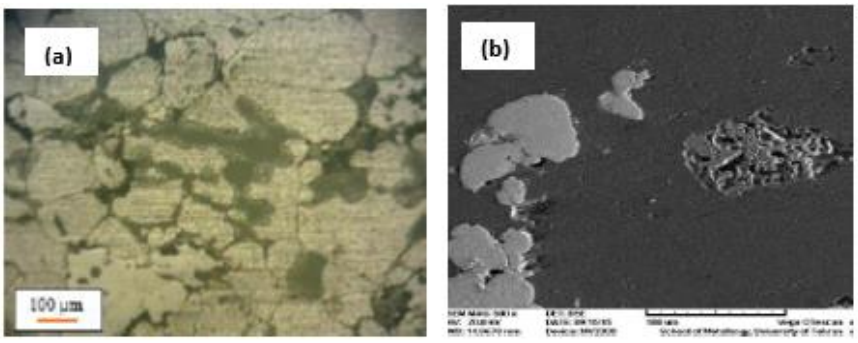

Fig. 5- a): OM and b): SEM micrographs of the Al-15wt.% Ni sample sintered at 640˚C for 75 minutes.

presented for comparison. As was expected the hardness of the reference sample was unaffected by the sintering time. The slightly higher hardness of the sample sintered for 15 min as compared to its reference sample counterpart is partially attributed to the presence of 15 wt.% Ni with 70 BHN in this sample which is harder than the base alloy having 24 BHN [27]. The increased hardness by increasing the sintering time to 30 min is attributed to formation a low quantity of eutectic compound and creation of a certain amount of hard Al_3Ni phase in this sample. However, this small amount of eutectic could not be detected in the OM image of Fig. 4-b. Sintering for 45 min resulted in increased hardness due to increased volume fraction of hard Al_3Ni compound. This sample exhibited the maximum hardness value among this series of samples being twice of its reference counterpart. However, the increased sintering time beyond 45 min resulted in decreased hardness. According to Table 1, the increased sintering time is associated with increased porosity of the composites imposing detrimental effect on hardness. Therefore, the increased sintering time has two competing effect in (i) increasing hardness due to increased volume fraction of hard Al_3Ni compound and (ii) decreasing hardness due to increased porosity content. For sintering times shorter than 45 min. the first effect was dominant while for longer sintering times the detrimental effect of increased porosity was more influential and resulted in decreased hardness.

3.2. Optimization of the sintering temperature

In order to achieve complete reaction between Al and Ni during sintering, an Al/Ni powder compact containing 15wt.% Ni sintered at 655˚C for 15 min. The OM studies on the cross section of this sample confirmed complete eutectic transformation and no unreacted Ni was detected in its microstructure as shown in Fig.7. However, sintering at this

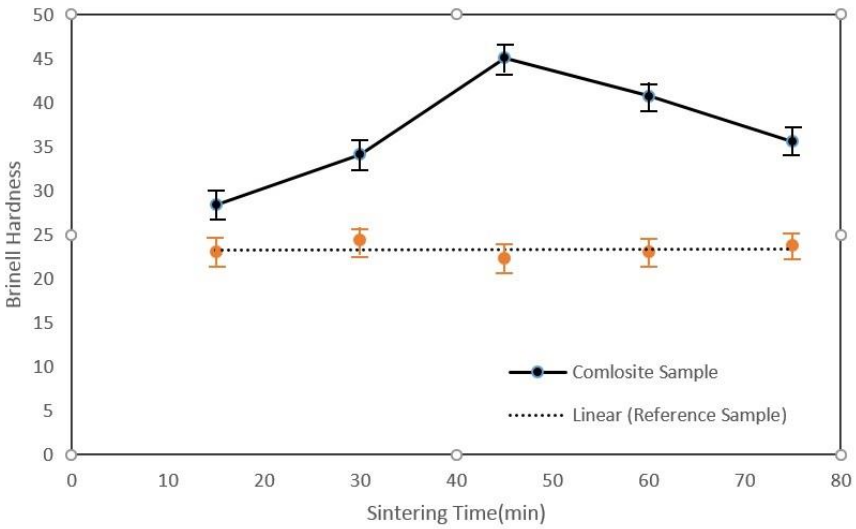

Fig. 6- The variation in Brinell hardness of Al-15wt.% Ni composites sintered at 640˚C for different times.

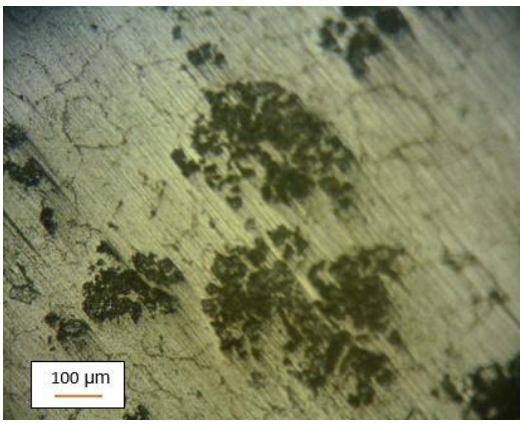

Fig. 7- Optical images of Al-15wt.% Ni samples sintered at 655˚C for 15 min.

relatively high temperature for longer periods of time (i.e. 30 min) resulted in partial melting and slight deformation of the sample.

3.3. Milling of the Ni powders

3.3.1 Optimization of milling time

Ball milling was conducted on irregular shaped Ni particles to increase their surface area and thereby increase their surface activity for gaining more effective reaction at the Al/Ni interface during sintering. For this purpose, in order to gain the required size and morphology, the Ni powders milled for different times and the milled powders were examined via SEM. The SEM micrographs of Ni powders milled for different times are shown in Fig. 8.

A comparison between Fig 8-a and Fig. 1-b reveals that 1.5h milling has altered the morphology of the powders in some extent. After 4h milling, most of the powders gained flaked shaped (Fig. 8-b). According to the Fig. 8-c milling for 6h created a complete flake shaped powders. According to previous studies [28], milling for longer periods of time results in fracturing of flakes and decreasing their size. Since the aim of this part of this study, is investigating the effect of powder morphology on the degree of reactions during sintering, it was necessary to use the same size range (63-125μm) for nickel powder, so milling for longer periods of time was avoided. Therefore, the milled Ni powders were sieved and the required size fraction (i.e.63-125μm) was treated with acetone, mixed with Al powders and cold pressed to be used for making composites.

3.3.2. Effect of Ni milling time on the microstructure of composites

The OM images of the polished cross section

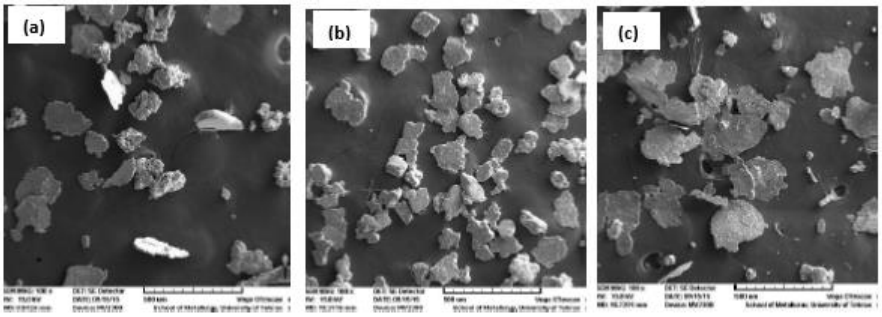

Fig. 8- SEM micrographs of Ni powders milled for different times, a:) 1.5h, b): 4h and c):6h.

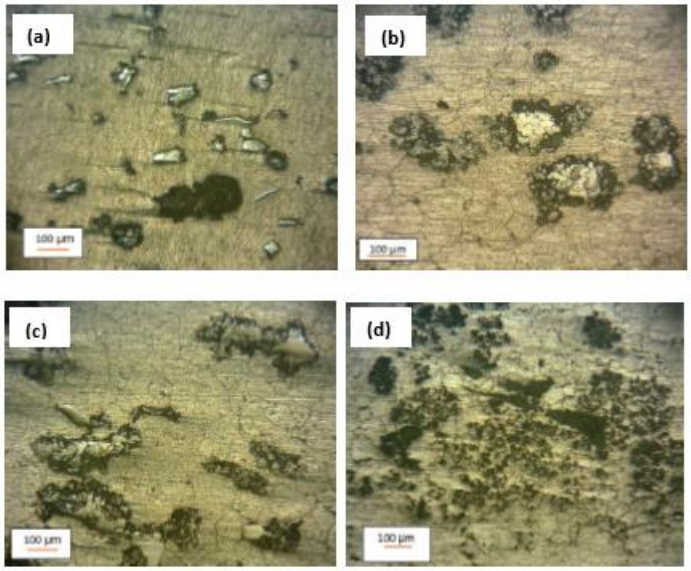

Fig. 9- OM images of the polished cross section of the Al-20wt.% Ni samples sintered at 655˚C for 15 min prepared from Ni particles milled for a): 0 min (un-milled), b): 1.5h, c): 4h and d); 6h.

of the Al-20wt.% Ni samples, prepared from Ni particles milled for different times and sintered at 655˚C for 15 minutes are shown in Fig 9.

Fig.9-a shows a number of un-reacted Ni particles. This result is in contrast with the result of sintering of the compact containing 15 wt.% of un-milled Ni particles and sintered at 655 ˚C for 15 min in which complete reaction between Al and Ni occurred as was shown in Fig.7. In fact, the increased Ni content to 20wt.% prohibited complete reaction as shown in the corresponding image of Fig.9-a. However, according to Fig.9-b, milling of Ni particles for 1.5h resulted in occurrence of some reaction at the Al/Ni boundaries. Fig.9-c shows that using the 4h milled Ni particles resulted in intensified eutectic reaction at the Al/Ni boundaries. The increased duration of milling for Ni particles to 6h resulted in complete reaction and no un-reacted Ni particle can be detected in the corresponding image of this sample (Fig.9-c).

The variation of the Brinell hardness of Al-20wt.% Ni samples, prepared from Ni particles milled for different times and sintered at 655˚C for 15 minutes are shown in Fig10. The increased hardness of composites with increased Ni milling time is attributed to increased amount of hard Al_3Ni phase generated during sintering due to more effective interaction between Al and Ni particles.

3.4. XRD results

The XRD patterns of three composite samples are presented in Fig. 11. The bottom pattern was

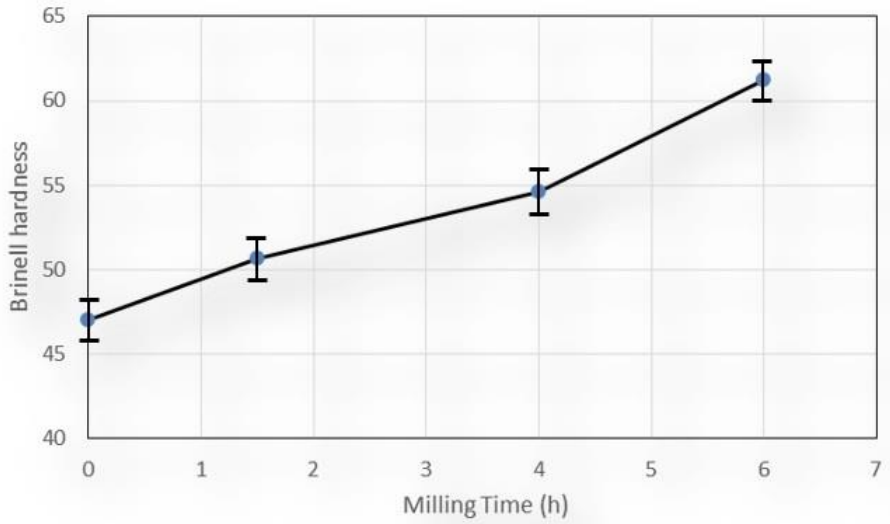

Fig. 10- The variation in Brinell hardness with Ni milling time of Al-20wt.% Ni composites sintered at 655˚C for 15 min.

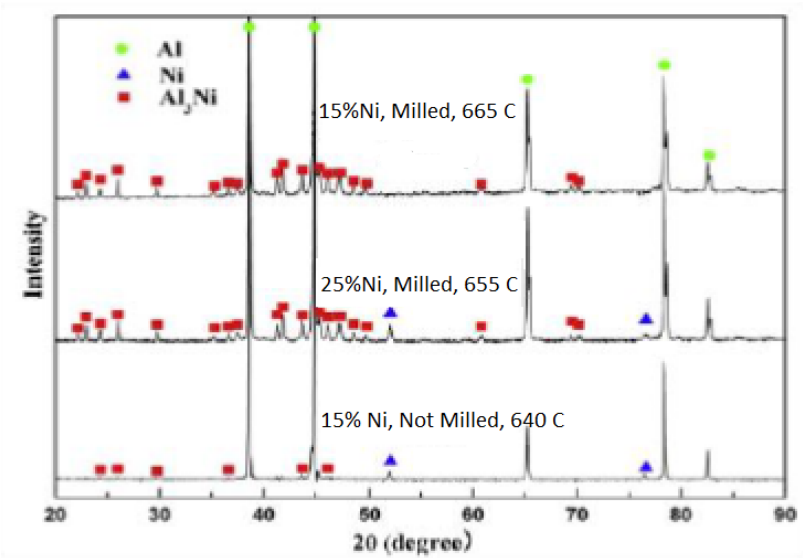

Fig. 11- XRD patterns of different samples sintered at various temperatures for 15 min.

taken from Al-15wt.% Ni sample that was prepared by un-milled Ni particles and was sintered at 640˚C for 15 min. As shown in the OM image of this sample (Fig. 3-a), effective reaction did not occurred during sintering so that its corresponding XRD pattern only shows Al and Ni peaks. The middle pattern of Fig. 11 was taken from Al-25wt.% Ni sample that was prepared by 6h milled Ni particles and was sintered at 655˚C for 15 min. In this pattern the characteristic peaks of Al_3Ni are observed indicating formation of this phase during sintering. However, due to relatively high concentration of Ni in the sample, a portion of un-reacted Ni remained in the sample as detected by XRD. The upper pattern is related to Al-15wt.% Ni sample that was prepared by using milled Ni particles and was sintered at 655˚C for 15 min. In this pattern, no Ni peak can be detected confirming the incident of complete reaction between Al and flake shaped Ni particles during sintering as was shown in the microstructure of this sample (Fig. 9-d).

4. Conclusions

In the present study Al-Al_3Ni composites prepared in situ by using powder metallurgy method. Specified amounts of Al and Ni powders were mixed, cold pressed and sintered at different temperatures for various times to find the optimum processing parameters for gaining the desired microstructure and properties. The following conclusions can be drawn from this investigation.

- Sintering at 640˚C of Al-15wt.%Ni compacts for more than 30 min and up to 75 min results in progressive formation of Al-Al_3Ni eutectic as a result of reaction between Al and Ni during sintering. The increased sintering time in the range of 15 to 75 min was accompanied by increased porosity of these composites. The increased sintering time up to 45 min resulted in increased hardness of these samples. However, sintering for longer times resulted in decreased hardness due to dominance of the detrimental effect of porosity. SEM studies of such a composite that was sintered at 640˚C for a relatively long period of time (i.e. 75 min) confirmed the presence of some un-reacted Ni particles.
- The OM studies on the cross section of a composite contained 15wt.% of Ni particles and sintered at 655 ˚C for 15 min revealed no un-reacted Ni particles. However, sintering at this relatively high temperature for longer periods of time, resulted in partial melting and slight deformation of the samples.
- In order to accelerate the reaction between Al and Ni during sintering, the Ni particles were subjected to ball milling and their irregular shape was converted to flakes. This operation increased their surface activity and resulted in more pronounced reaction between Ni and Al particles during sintering. The increased milling time of Ni particles from 1.5h to 6h resulted in progressive reaction between Ni flakes and spherical Al particles presented in Al-20wt.% Ni samples sintered at 655˚C for 15min. This was accompanied by the increased content of hard Al_3Ni phase and thereby continuous increased hardness of composites.
- The increased content of milled Ni to 25wt.% resulted in some unreacted Ni particles in the matrix of composite sintered at 655˚C for 15min as was confirmed by XRD studies.

References

1. Torralba J.M., Casta CE. and Velasco F. P/M Aluminum Matrix Composites: An Overview. Materials Processing Technology. 2003; 133, 203-206.
2. Shabani A., Toroghinejad M.R. and Shafyei A. Fabrication of Al/Ni/Cu composite by accumulative roll bonding and electroplating processes and investigation of its microstructure and mechanical properties. Materials Science & Engineering A. 2012; 558, 386–393.
3. Liu J.B., Wang L.M. and Jiang J. Sh. Al2Cu/α-Al composite coating prepared by plasma surface metallurgy. Materials Letters. 2008; 62, 1569–1571.
4. Tjong S. C. and Ma Z.Y. Microstructural and mechanical characteristics of in situ metal matrix composites. Material Science and Engineering. 2000; 29, 49-113.
5. Shi Z. and Yong J.M. The Interfacial Characteristics of Oxidized SiCp/2014 Al Composites. Materials Science and Engineering A. 2001; 41, 46-53.
6. Lee J.C. and Ahn J.P. Control of the Interface in SiC/Al Composites. Scripta Materialia.1999; 41, 895-900.
7. Flemigs M.C. Solidification Processing. McGraw-Hill; 1974.
8. Hsu C.J., Kao P.W. and Ho N.J. Ultrafine-grained Al–Al_2Cu composite produced in situ by friction stir processing. Scripta Materialia. 2005; 53, 341–345.
9. Das K., Bandyopadhyay T. K. and Das S. A review on the various synthesis routes of TiC reinforced ferrous-based composites. Journals of Materials Science. 2002; 37, 3881-3892.
10. Emamy M., Vaziri Yeganeh S.E., Razaghian A. and Tavighi K. Microstructures and tensile properties of hot-extruded Al matrix composites containing different amounts of Mg2Si. Materials Science & Engineering A, 2013; 586, 190–196.
11. Tavighi K., Emamy M. and Emami A.R. Effects of extrusion temperature on the microstructure and tensile properties of Al–16 wt.% Al_4Sr metal matrix composite. Materials and Design. 2013; 46, 598-604.
12. Zare-Bidaki A. and Akhlaghi F. Influence of graphite content on the dry sliding and oil impregnated sliding wear behavior of Al 2024-graphite composites produced by in situ powder metallurgy method. Wear, 2009; 266, 37-45.
13. Aravind M., Yu P., Yau M.Y. and Dickon H.L. Formation of Al2Cu and AlCu intermetallics in Al(Cu) alloy matrix composites by reaction sintering. Materials Science and Engineering A. 2004; 380, 384–393.
14. Yu P., Deng Ch. J., Ma N.G, Yau M.Y and Dickon H.L. Formation of nanostructured eutectic network in α-Al2O3 reinforced Al–Cu alloy matrix composite. Acta Materialia, 2003; 51, 3445–3454.
15. Rasouli M., Ghazi Asgar M., Akhlaghi F. and Marjani O. Preparation of $AlAl_2Cu$ Composites In-situ Processed via Reactive Infiltration. Metallography, Microstructure and Analysis. 2022; 11, 634-648.
16. Anvari S. Z., Enayati M.H.and Karimzadeh F. Wear Behavior of Al-Al_3V and Al-(Al_3V-Al_2O_3) Nanostructured Composites

Fabricated by Mechanical Alloying and Hot Extrusion. Journal of Ultrafine Grained and Nanostructured Materials, 2020; 53(2), 135-145.
17. Gostariani R., Asadi Asadabad M. and Ebrahimi R. The effect of Al-BN Powder Preparation Method on Tensile Properties of Extruded bulk Nanocomposite. Journal of Ultrafine Grained and Nanostructured Materials, 2022; 55(1), 70-77.
18. Mashayekhi F. and Akhlaghi F., Effect of some processing parameters on microstructure and hardness profiles of Al-Al_2Cu functionally graded materials prepared in-situ via interaction between molten Al and solid Cu. Journal of Ultrafine Grained and Nanostructured Materials, 2024; 57(1), 35-47.
19. Qian J., Li J., Xiong J., Zhang F. and Lin X. In situ synthesizing Al_3Ni for fabrication of intermetallic- reinforced aluminum alloy composites by friction stir processing. Materials Science and Engineering, 2012; 5, 279-285.
20. Lieblich M., Gonzalez-Carrasco J.L. and Garcia-Cano F. Asymmetrical phase growth in a PM Al/Ni_3Al composite. Journal of materials science letters.1999; 18, 905-908.
21. Lieblich M., Gonzalez-Carrasco J.L. and Caruana G. Thermal stability of an Al-Al_3Ni composite processed by powder metallurgy. intermetallics, 1997; 5, 515-524.
22. Rasouli M., Akhlaghi F., Ogo O.O. and Paidar M. Preparation and characterization of in-situ Al-Al_XNi_Y composites via reactive infiltration. Journal of Alloys and Compounds. 2019; 780, 829-845.
23. Kim J., Soprunyuk T.V., Chawake N., Zheng Y.H., Spieckermann F., Hong S.H., Kim K.B. and Eckert J. Outstanding strengthening behavior and dynamic mechanical properties of in-situ Al–Al_3Ni composites by Cu addition. Composites Part B, 2020; 189, 1-14.
24. Balakrishnan M., Dinaharan I., Kalaiselvan K. and Palanivel R. Friction stir processing of Al_3Ni intermetallic particulate reinforced cast aluminum matrix composites: Microstructure and tensile properties. Journal of Materials Research and Technology. 2020; 9(3), 4356-4367.
25. Rana R.S., Purohit R. and Das S. Review of recent studies in Al matrix composites. Int. J. Scientific & Engineering Research. 2012; 3(6), 60- 83.
26. Mosleh-Shirazi S. and Akhlaghi F. The impact of matrix microstructure and reinforcement size (micron vs. nano-size) on the compressibility of Al-SiC powder mixtures and hardness of Al/SiC composites. Journal of Ultrafine Grained and Nanostructured Materials, 2022; 55(2), 133-144.
27. ASM Handbook, Properties and selection: Nonferrous Alloys and Special- Purpose Materials, American Society for Metals, Metals Park, OH, 1998, 10th Edition. P.62-152.
28. Akhlaghi F., Khakbiz M. and Rezaii Bazazz A. Evolution of the size distribution of Al-B_4C nanocomposite powders during mechanical milling: a comparison of experimental results with artificial neural networks and multiple linear regression models. Neural Computing and Applications. 2017; 31, 1-10.